Multi-scale Analysis of InSAR Time Series to Estimate Variations in Topographically Correlated Propagation Delays

Yu-nung Nina Lin[1], Mark Simons[1], Eric Hetland[1], Pablo Muse[2], and Christopher DiCaprio[1]

1. Devision of Geological and Planetary Sciences, California Institute of Technology 2. Dept. of Signal and Image Processing, Facultad de Ingeniera, Universidad de la Republica, Uruguay

Introduction

We use InSAR to measure changes in distance across an image between a satellite and the ground. With the aim to detect tectonic deformation, many InSAR observations are plagued by temporally changing propagation delays that correlate with topographic variations. These delays are frequently termed tropostatic delays and are assumed to result from temporal variations in vertical stratification of the troposphere. Assuming a linear model between topography and phase, we present a robust approach to estimating a transfer function K which is relatively insensitive to confounding processes (e.g., earthquake deformation, phase ramps from orbit errors, etc). Our approach takes advantage of a multi-scale perspective by adopting a band-pass decomposition of both topography and observed phase. By decomposing topography and observed phase in a given interferogram into several spatial scales, we determine the bands spanning different characteristic length scales wherein correlation between topography and phase is significant and stable. Our approach also uses the inherent redundancy provided by multiple interferograms constructed with common scenes. We define a unique set of component time intervals, T_{int}, using a suit of interferometric pairs. The ensemble of pair-based K_{pair} are then combined to estimate a temporally consistent K for each time interval (K_{int}). Internally consistent K_{pair} values can then be predicted from these K_{int} values to correct each interferogram. We test our approach in the region of Makran subduction zone. We infer large temporal variations in the K values. The tropostatic correction only accounts for a relatively small portion of the observed phase, which implies that in the future we need to consider more complex atmospheric models in this

Low Amplitude Tectonic Signals

Low amplitude tectonic signals, such as those related to interseismic strain accumulation, are easily obscured by other non-tectonic signals including atmospheric disturbance in SAR observations. Our specific target is the Makran subduction zone where a M 7.9 earthquake occurred in 1945. The large magnitude of this event implies we should eventually be able to detect the effects of coupling on the subduction interface.

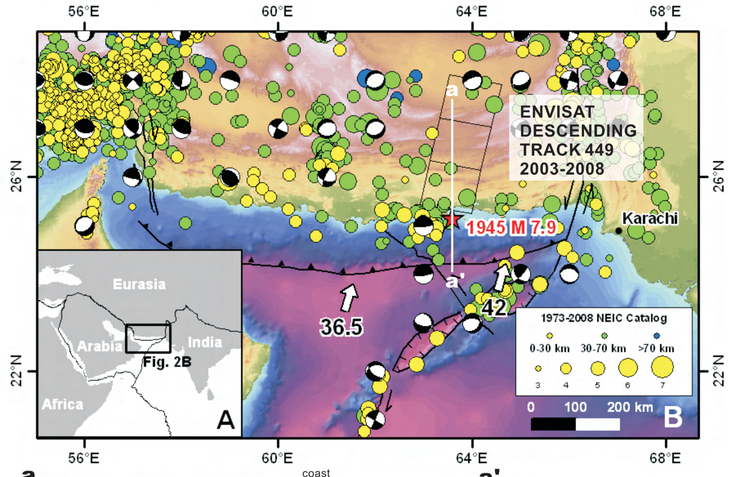

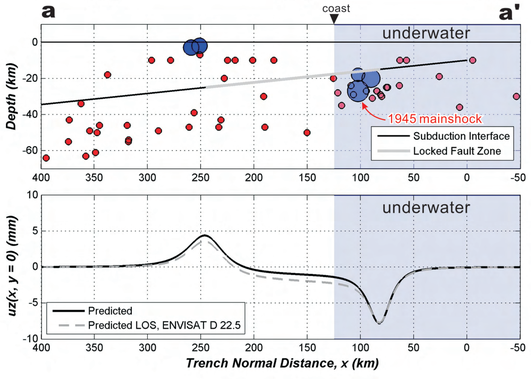

Back-slip model predicts that the interseismic uplift rate is as low as 5 mm/yr.

$\theta = 3.5^{\circ}$
D1 = 15 km
D2 = 25 km (Byrne & Sykes, 1992)
Plate Convergent Rate:
42 mm/yr (DeMets et al., 1990)

To properly estimate the interseismic strain from interferograms, we try to correct for tropospheric phase delays first.

Tropostatic Correction

Tropospheric perturbations can be divided into two types: static vertical stratification and turbulent mixing (Hanssen, 2001). Phase delay resulted from the former is due to temporal changes of water vapor distribution in zenith direction and is usually correlated with topography. In many cases, correction on this static component is sufficient to remove first order tropospheric signals.

Static Vertical Stratification ("Tropostatic")

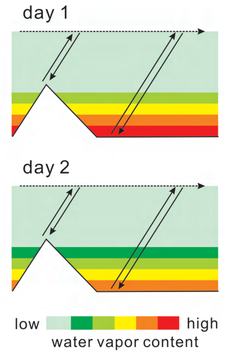

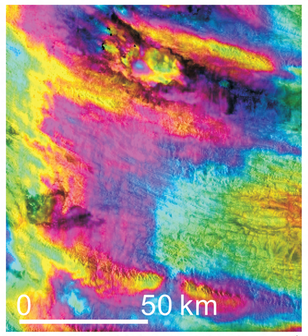

(Makran subduction zone)

Turbulent Mixing

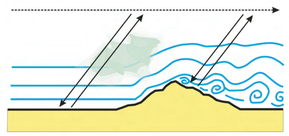

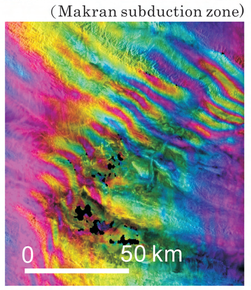

(Makran subduction zone)

Physical Models (tropostatic delay only)

$$\Delta L = \frac{10^{-6}}{\cos\theta}\int_h^H N(z)dZ$$

$$N(z) = 77.6\frac{P(z)}{T(z)} + 3.73 * 10^5\frac{e(z)}{T^2(z)} \quad \textit{(Bean and Dutton, 1966)}$$

$$\Delta L = \frac{2.27 * 10^{-3}P_g + \nu U_g 10^{\gamma(T_g - 273)}}{\cos\theta} \quad \textit{(Delacourt et al., 1998)}$$

ΔL: excess path in line of sight direction
N: refractivity
ν, γ: constants
P_g, T_g, U_g: ground-based meteorological data

Multi-scale Analysis of Tropostatic Delays

A study in the region of Lake Mead (Cavalié et al., 2007) shows that tropostatic phase delay can be approximated by

$$\phi = b + Kh$$

b : bias term
K : transfer function
h : topographic relief

If this linear approximation holds, the K value should stay constant regardless of topographic wavelength. Therefore, we can take advantage of the multi-scale perspective to robustly estimate a spatially constant K which is less sensitive to other confounding processes. The coherence/incoherence between topography and phase at different length scales (see next panel) may also help determine at which length scales the tropostatic phase delay signals are dominant.

$$\phi(\lambda) = b_{pair} + K_{pair}h(\lambda)$$

Linear Approximation between phase and topographic relief

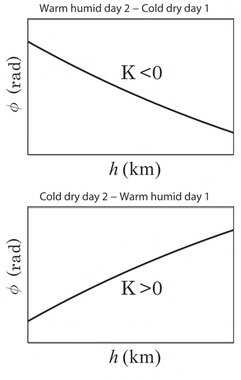

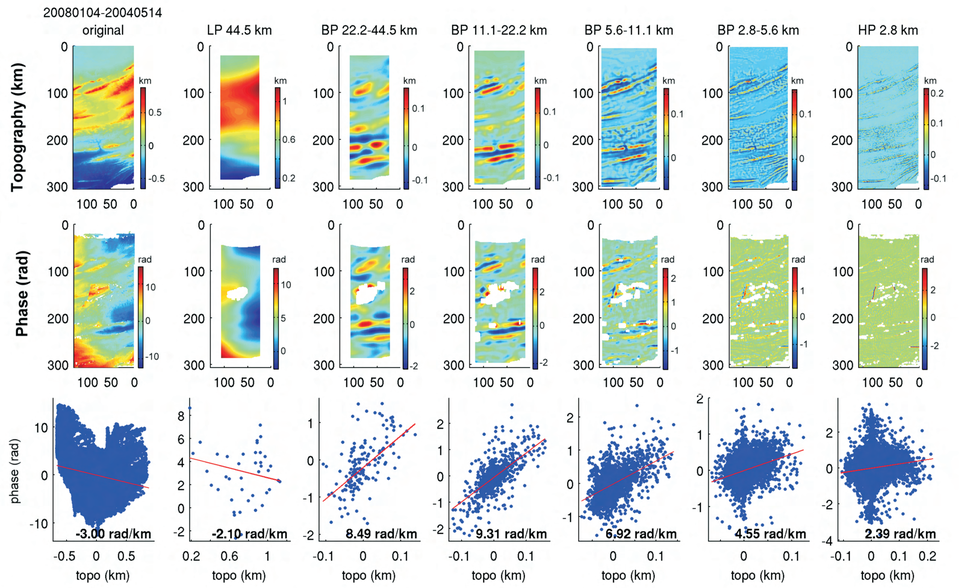

▲ The original and decomposed topography and interferogram. Each channel is sampled based on Nyquist frequency to form the scatter plot. The four band-passed channels show higher coherency between topography and phase and more consistent K (the slope in scatter plots). LP: low pass; BP: band pass; HP: high pass.

▼ The K_{pair} value of this specific pair is determined by L1-regression, using all the Nyquist-sampled data points from the four band-passed channels.

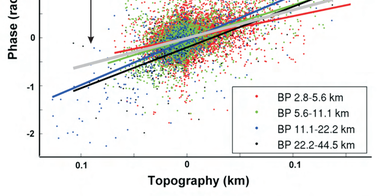

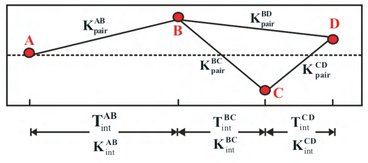

◀ Multiple interferograms constructed from one same SAR image (such as B) can provide redundant information

▼ We can correct the interferogram by using the predicted K_{pair} values from the K time series.

Time Series of K Values

After determining K_{pair} for each interferogram, we use the inherent redundancy provided by multiple interferograms to determine an internally consistent set, K_{int}. Each K_{pair} is then the linear combination of K_{int} values. This two-step linear regression can also be further combined into a single step:

Two Step Inversion → **One Step Inversion**

$$\phi(\lambda) = b_{pair} + K_{pair}h(\lambda)$$
$$[G][K_{int}] = [K_{pair}]$$

$$\begin{bmatrix} h_1(\lambda_1) & 1 & 0 & 0 & 0 & 0 & \cdots & 0 \\ h_1(\lambda_2) & 1 & 0 & 0 & 0 & 0 & \cdots & 0 \\ \vdots & \vdots & \vdots & \vdots & \vdots & \vdots & \cdots & 0 \\ h_1(\lambda_n) & 1 & 0 & 0 & 0 & 0 & \cdots & 0 \\ \vdots & \vdots & \vdots & \vdots & \vdots & \vdots & \cdots & 0 \\ 0 & 0 & h_{m-1}(\lambda_1) & 1 & h_{m-1}(\lambda_1) & 1 & \cdots & 0 \\ 0 & 0 & h_{m-1}(\lambda_2) & 1 & h_{m-1}(\lambda_2) & 1 & \cdots & 0 \\ \vdots & \vdots & \vdots & \vdots & \vdots & \vdots & \cdots & 0 \\ 0 & 0 & 0 & 0 & \cdots & \cdots & h_m(\lambda_n) & 1 \end{bmatrix} \begin{bmatrix} K_{int}^1 \\ b_{int}^1 \\ K_{int}^2 \\ b_{int}^2 \\ \vdots \\ K_{int}^p \\ b_{int}^p \end{bmatrix} = \begin{bmatrix} \Delta\phi_1(\lambda_1) \\ \Delta\phi_1(\lambda_2) \\ \vdots \\ \Delta\phi_1(\lambda_n) \\ \vdots \\ \Delta\phi_{m-1}(\lambda_1) \\ \Delta\phi_{m-1}(\lambda_2) \\ \vdots \\ \Delta\phi_m(\lambda_n) \end{bmatrix}$$

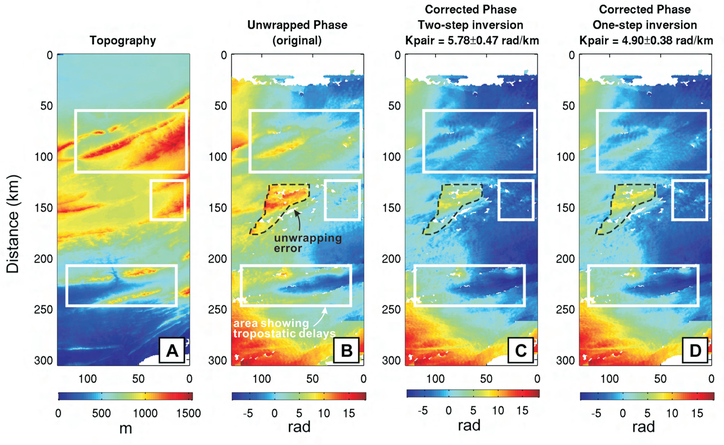

K Time Series

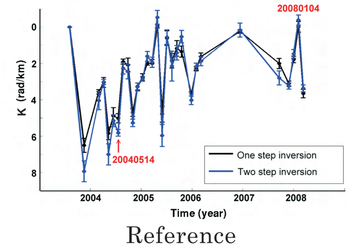

Reference

Bean, B., and E. Dutton, *Radio meteorology*, Monography, Natl. Bur. of Stand., Gaithersburg, 1966.

Byrne, D. E., and L. R. Sykes, Great thrust earthquakes and aseismic slip along the plate boundary of the Makran subduction zone, *J. Geophys. Res., 97*, 449–478, 1992.

Cavalié, O., M.-P. Doin, C. Lasserre, , and P. Briole, Ground motion measurement in the Lake Mead area, Nevada, by differential synthetic aperture radar interferometry time series analysis: Probing the lithosphere rheological structure, *J. Geophys. Res.*, B03403, doi:10.1029/2006JB004344, 2007.

Delacourt, C., P. Briole, and J. Achache, Tropospheric corrections of SAR interferograms with strong topography. Application to Etna, *Geophys. Res. Lett., 25*, 2849-2852, 1998.

DeMets, C., R. G. Gordon, D. F. Argus, and S. Stein, Current plate motions, *Geophys. J. Int., 101*, 425–478, 1990.

Hanssen, R. F., *Radar Interferometry, Data Interpretation and Error Analysis*, Springer, New York, 2001.

Acknowledgment

We would like to thank European Space Agency (ESA) for supplying ENVISAT images through a category 1 project. We also thank Sebastien Leprince for the help in clarifying concepts.